CONF-9

CONF-901116--10

DE91 000706

Photodetachment of Metastable He^-

J. S. Thompson,* D. J. Pegg,† and J. Dellwo
Department of Physics, University of Tennessee, Knoxville TN, 37996, USA

R. N. Compton‡ and G. D. Alton
Oak Ridge National Laboratory, Oak Ridge TN, 37831, USA

A crossed-beams apparatus has been used to measure angular distributions and cross sections for photoelectron detachment from metastable He^-. Energy- and angle-resolved electron spectroscopy was used to investigate the spectral dependences of the angular distribution of the photoelectrons. The angular distributions along with photoelectron yield measurements were used to determine the cross sections for photodetachment of $He^-(2^4P)$ via the energy resolved $He(2^3P)$ and $He(2^3S)$ exit channels. The precision of the cross section measurements was enhanced by exploiting the kinematic effects associated with detachment from a fast beam source. Calculated cross sections for the photodetachment of H^- were used to establish an absolute scale for the He^- cross section measurements.

*Present Address: Joint Institute for Laboratory Astrophysics of the University of Colorado and the National Institute of Standards and Technology, Boulder, CO 80309, USA.

†Also with: Physics Division, Oak Ridge National Laboratory, Oak Ridge, TN 37831-6377, USA.

‡Also with: Department of Chemistry, University of Tennessee, Knoxville, TN 37996, USA.

I. INTRODUCTION

In this paper we report on our photodetachment studies of the metastable He^- ion. Photoelectron angular distributions, and angular differential and integral cross sections have been measured using a crossed laser-ion beams technique. The experiment exploits the advantages associated with forward-directed energy spectroscopy of electrons detached from a fast beam source.

The He^- ion is the prototype of an unusual class of unstable, yet long-lived, negative ions. He^- is formed in the spin-aligned (1s2s2p) ^{4}P state (see Fig. 1) when an electron is captured by an He atom in the (1s2s) ^{3}S state. This spin-aligned quartet state is metastable since it is embedded in a doublet continuum. As a result, the allowed autodetachment process induced by the strong electrostatic interaction among the electrons is forbidden. Thus the ^{4}P state decays via the forbidden autodetachment process induced by the relatively weak spin-dependent interactions. The varying strengths of these interactions result in a differential metastability among the fine structure levels. Lifetimes of the J=$\frac{1}{2}, \frac{3}{2}, \frac{5}{2}$ levels have been measured[1] to be 16, 10 and 500 μsec, respectively. Metastable He^- ions are sufficiently long lived that they undergo very little exponential depletion by autodetachment prior to photodetachment in the present crossed-beams apparatus. Small corrections to the measured photoelectron yields ($\sim$ 2%) are, however, made to account for the unstable nature of this ion. The structure of He^- is now well established. The electron affinity of He(2^3S) has been calculated by Bunge and Bunge[2] to be 77.51$\pm$0.04 meV and was first measured by Brehm, Gusinow and Hall[3] using crossed laser-ion beams photoelectron spectroscopy and later by Peterson, Bae and Huestis[4] using a merged-beams threshold photodetachment technique.

When the $He^-(2^4P)$ ion interacts with visible radiation, two competing photodetachment channels into the continuum are open:

$$h\nu + He^-(2^4P) \longrightarrow He(2^3S) + e^-(ks, d) \tag{1}$$

$$h\nu + He^-(2^4P) \longrightarrow He(2^3P) + e^-(kp). \tag{2}$$

In an independent electron description of process 1, a p-orbital electron is photodetached resulting in an electron represented by an admixture of outgoing s- and d-waves. In process 2, an s-orbital electron is photodetached, leading to a pure outgoing p-wave in the independent electron model. In this paper, photodetachment processes will frequently be referred to by the final state of the atom.

II. EXPERIMENTAL TECHNIQUE

The technique of energy- and angle-resolved photoelectron spectroscopy has been used to investigate the interaction of negative ions and radiation. Cross sections for photodetachment are determined from measurements of the yields and angular distributions of photoelectrons ejected from the ions at the interaction site of the crossed laser and negative ion beams. Fig. 2 is a schematic diagram of the crossed-beams apparatus. A fast moving ($v \sim 10^8$ cm/sec) and tenuous beam ($\rho \sim 10^3$ ions/cm^3) of He^- ions is crossed perpendicularly by an energy-resolved and linearly-polarized beam of photons from a pulsed dye laser. As a result of the photon-ion interaction, precisely known amounts of energy and angular momentum are transferred to the ion. Following photodetachment events, electrons ejected in the field-free interaction region in the direction of motion of the ion beam (forward-directed electrons) are collected, energy analyzed and detected. A typical photoelectron spectrum is shown in Fig. 3.

The negative ion beam source is produced by double charge transfer (sequential electron capture) when a momentum-selected positive ion beam from an accelerator is passed through a Li vapor charge-exchange cell. The beam exiting the cell is charge state analyzed after a travel time of a few microseconds. The negative ion component ($\lesssim 1$ %) is then deflected by 10° into a beam line containing an electron spectrometer consisting of a spherical-sector energy analyzer and a channeltron electron multiplier detector. The ion beam is crossed with the laser beam approximately 2 mm in front of the entrance to the electron spectrometer. Sets of apertures are used to ensure that the overlap of the two beams remains unaltered during the measurements. The flashlamp-pumped pulsed dye laser used for this investigation has a maximum repetition rate of 10 Hz and a pulse duration of 2.2 μsec. The output power of the laser was carefully chosen to avoid saturation of each of the photodetachment processes studied. Further details of the apparatus can be found in a paper by Pegg[5].

As a consequence of the fast moving and unidirectional nature of the source, the kinematic energies, yields, energy distributions and angular distributions of the photoelectrons detached from the moving ions will be modified by kinematics. The combination of a fast-moving beam source and forward-directed collection used in the present experiment permits one to effectively exploit kinematic effects such as spectral peak shifting and line doubling. The kinematically-shifted energy of a forward-directed ($\theta_L = 0$) electron in the laboratory frame, E_L, is related to its energy in the ion frame by the relationship $E_L = ME_C$, where M represents a kinematic "magnification" factor, $M = \left(1 \pm \sqrt{\epsilon/E_C}\right)^2$. Here, ϵ is the energy of an electron moving with the same velocity as the ions in the beam. The positive sign in the factor M corresponds to emission of electrons in the forward direction ($\theta_C = 0$) in the ion frame and the

negative sign corresponds to backward-directed ($\theta_C = \pi$) emission in the ion frame. If the ion beam velocity exceeds the velocity of the detached electron in the ion frame, both forward- and backward-directed electrons will be swept forward in the laboratory frame. Kinematic peak doubling arises since E_L becomes double valued in this case. The laboratory energy separation of the twin peaks is $\Delta E_L = 4\sqrt{\epsilon E_C}$. Details of these and other kinematic modifications have been previously reported[6].

III. RESULTS

In this section we describe measurements of photoelectron angular distributions and photodetachment cross sections. An absolute scale for the cross section measurements is established using known photodetachment cross sections for H^-.

A. Angular Distributions

The apparatus described in this paper was designed so that the negative ion and photon beams crossed perpendicularly. The electron spectrometer was placed in the path of the negative ion beam such that it collected only those photoelectrons ejected in the forward direction in the laboratory frame. In this geometry the angular correlation factor, f(θ), for electrons photodetached by linearly polarized light is

$$f(\theta) = 1 + \beta P_2(\cos\theta). \tag{3}$$

In this equation, θ is the angle between the emission direction of the photoelectron and the polarization vector of the incident light, β is an asymmetry (anisotropy) parameter and $P_2(\cos\theta)$ is the second-order Legendre polynomial. The asymmetry parameter completely characterizes the shape of the angular distribution of the photoelectrons.

The angular distribution of electrons photodetached from He^- was investigated by taking electron energy spectra at various angles between the photoelectron emission direction and the linear polarization vector of the laser beam. The angle was changed by rotating the polarization vector relative to the fixed photoelectron collection direction. The angular distribution measurement technique has been tested, at several different wavelengths in the visible, by photodetaching beams of H^- and Li^- ions. The predicted $\cos^2\theta$ ($\beta = 2$) distribution was obtained in all cases.

The He^- ion is a reasonably simple system for probing the effects of correlation on electron emission following photodetachment. Experimental results for photodetaching He^- into the ^3S and ^3P exit channels are listed in Table I. A recent calculation[7] is in essential agreement with the present angular distribution results. A detailed description of the experiment and an analysis of the data is given in a previous paper[8].

B. Photodetachment Cross Sections

The partial (angular integral) cross sections, $\sigma(^3S)$ and $\sigma(^3P)$, for photodetaching electrons from $He^-(2^4P)$ via the $He(2^3S)$ and the $He(2^3P)$ exit channels, respectively, have been measured relative to the cross section, $\sigma(^2S)$, for photodetaching D^- via the $D(1^2S)$ exit channel.

The angular integral cross section, $\sigma(x)$, for photodetachment of an ion via an exit channel labeled x can be expressed in terms of the yield of photoelectrons, Y(x), ejected in the direction of the linear polarization vector of the light beam in the following manner:

$$\sigma(x) = \frac{4\pi Y(x)}{[1+\beta(x)]g(x)\phi(x)\kappa(x)\rho(x)(\Delta\Omega)VGT}. \tag{4}$$

In this expression, β is the asymmetry parameter characterizing the shape of the emission pattern, g is the frame-transformed solid angle ratio, k represents the photoelectron collection and detection efficiency, ρ is the ion beam density, ϕ is the photon flux, V is the interaction volume, $\Delta\Omega$ is the solid angle defined by the collection geometry, G measures the spatial overlap of the two crossed beams, and T is the integration time for each yield measurement. In the present work, relative cross sections are obtained by comparing, under identical geometric conditions, the yields of electrons produced in the photodetachment of ions of interest, Y(x), and a reference ion, Y(r), whose cross section is known. Thus the relative cross sections for the two photodetachment processes can be written as

$$\frac{\sigma(x)}{\sigma(r)} = \frac{Y(x)\rho(r)\phi(r)g(r)[1+\beta(r)]}{Y(r)\rho(r)\phi(r)g(x)[1+\beta(x)]}. \tag{5}$$

Here the measured yield ratio is multiplied by several measured factors in order to account for the different frame-transformed solid angles, photon fluxes, ion densities, and asymmetry parameters associated with photodetaching electrons from the two beams. All geometric factors, being equal, cancel in the equation. In this work it is arranged by appropriate choice of beam energies, that the photoelectron energy peaks in each spectra are kinematically shifted so they coincide in energy in the laboratory frame. The efficiency factors, k(x) and k(r), associated with collection and detection of photoelectrons at the same laboratory energy from the ions of interest and the reference ions, will then cancel in the equation. The ion beam densities, ρ, and the solid angle transformation factors, g, both depend on the velocity of the ion beams. This quantity can be determined very precisely ($\sim 0.1\%$), in situ, by simply analyzing the photoelectron spectra. Details of the experiment have been discussed previously by Pegg *et. al.*[9].

The partial cross section ratios, $\sigma(^3S)/\sigma(^2S)$ and $\sigma(^3P)/\sigma(^2S)$, have been measured at photon energies of 1.781, 1.946, and 2.091 eV. The results are $\sigma(^3S)/\sigma(^2S)$= 0.60 ± 0.02 (1.781 eV), 0.57 ± 0.04 (1.946 eV), and 0.49 ± 0.04 (2.091 eV); $\sigma(^3P)/\sigma(^2S)$ $= 0.28 \pm 0.02$ (1.781 eV), 0.18 ± 0.02 (1.946 eV), and 0.12 ± 0.01 (2.091 eV). The uncertainties quoted on these values represent two standard deviations of the weighted mean of several data sets each comprising a number of individual spectra added together. A scale for the relative cross section measurements can be readily established by assuming theoretical values for the $\sigma(^2S)$ cross section for photodetaching the D^- ion. Several calculations of H^- photodetachment cross sections have been made and can be used for this purpose. The pertubation-variation results of Stewart[10] have been arbitrarily chosen for the purpose of normalization in the present work. Combining the theoretical values (assuming a 3% uncertainty) with the measured cross section ratios produces the partial cross sections (in Mb) shown in Table II. The sum of the partial cross sections, σ_{total}, are also tabulated.

Theoretical total cross section calculations[7,11,12] and the sum of the of the present partial cross section measurements are in good agreement at all photon energies used in the experiment. The less precise total cross section measurements of Compton, Alton and Pegg[13], and Hodges, Coggiola and Peterson[14] are in essential agreement with the sum of the partial cross sections measured here. At the present time, however, there are no other experimental or theoretical results available for comparison with our measured partial cross sections.

IV. SUMMARY

A crossed-beams apparatus that employs energy- and angle-resolved electron spectroscopy has been used to measure angular distributions of photoelectrons and angular and integral cross sections for the photodetachment of He^-. An absolute scale has been established by making relative photoelectron yield and angular distribution measurements of He^- ion beams and D^- reference ion beams whose photoelectron angular distribution and photodetachment cross section are known. The relatively high precision ($\sim$ 5% in favorable cases) of the present cross-section ratio measurements, reflects our ability to exploit, in a novel way, certain kinematic effects associated with a fast moving source of ions and simultaneous collection of electrons in the forward direction. These features of the present apparatus have not been used in previous photodetachment studies.

ACKNOWLEDGMENTS

Three of us (JST, DJP and JD) acknowledge research support from the US Department of Energy, Office of Basic Energy Sciences, Division of Chemical Sciences through the University of Tennessee. Oak Ridge National Laboratory is operated by Martin Marietta Energy Systems, Inc. under contract No. DE-AC05-84OR21400.

---

[1]R. Novick and D. Weinflash, **Precision Measurement and Fundamental Constants, Proc. Int. Conf., Natl. Bur. Stds.**, Gaithersburg MD, August 3-7, 1970, NBS Special Pblication 343, pp. 403-410.

[2]A. V. Bunge and C. F. Bunge, Phys. Rev. A **9**, 452 (1979).

[3]B. Brehm, M. A. Gusinow and J. L. Hall, Phys. Rev. Lett. **19**, 737 (1967).

[4]J. R. Peterson, Y. K. Bae and D. L. Huestis, Phys. Rev. Lett. **55**, 692 (1985).

[5]D. J. Pegg, **The Physics of Electronic and Atomic Collisions**, A. Dalgarno, R. Freund, P. Koch, M. Lubell and T. Lucatorto Eds (American Inst. of Physics, N.Y., 1989) pp. 233-240.

[6]D. J. Pegg, J. S. Thompson,R. N. Compton and G. D. Alton, Nucl. Instrum. Meth. **B 40/41**, 22 (1989).

[7]H. P. Saha and R. N. Compton, Phys. Rev. Lett. **64**, 1510 (1990).

[8]J. S. Thompson, D. J. Pegg, R. N. Compton and G. D. Alton, J. Phys. B **23**, L15 (1990).

[9]D. J. Pegg, J. S. Thompson, J. Dellwo, R. N. Compton and G. D. Alton, Phys. Rev. Lett. **64**, 278 (1990).

[10]A. L. Stewart, J. Phys. B **11**, 3851 (1978).

[11]A. U. Hazi and K. Reed, Phys. Rev. A **24**, 2269 (1981).

[12]L. V. Chernysheva, G. F. Gribakin, V. K. Ivanov and M. Vu. Kuchiev, J. Phys. B **21**, L419 (1988).

[13]R. N. Compton, G. D. Alton and D. J. Pegg, J. Phys. B **13**, L651 (1980).

[14]R. .V. Hodges, M. J. Coggiola and J. R. Peterson, Phys. Rev. A **23**, 59 (1981).

TABLE I. Asymmetry parameter, β, for the ^3S and ^3P exit channels of He^-.

Exit Channel	Photon Energy (eV)					
	2.456	2.224	2.087	1.942	1.870	1.775
^3S	1.35±0.02	1.63±0.05	1.31±0.07	1.28±0.02	1.23±0.02	1.15±0.02
^3P	$2.00\pm{}^{0.00}_{0.03}$	1.74±0.03	1.53±0.05	1.59±0.03	1.52±0.03	1.52±0.04

TABLE II. Photdetachment cross sections for He^- (Mb).

	Photon Energy (eV)		
	1.781	1.946	2.091
$\sigma(^3S)$	22.9±1.0	20.5±1.5	16.6±1.8
$\sigma(^3P)$	10.0±0.6	6.7±0.6	4.1±0.4
σ_{total}	32.9±2.4	27.2±3.1	20.7±3.0

FIG. 1. Partial energy level diagram for the He and He^- systems. The He^- ion exists in the metastable $(1s2s2p)\ ^4P$ state.

FIG. 2. A schematic view of the crossed laser-ion beams apparatus used in the energy- and angle-resolved photoelectron spectroscopy measurements.

FIG. 3. Energy spectrum of electrons photodetached from a 40 keV beam of He^- ions at $\lambda = 689.5$ nm. Peaks 1 and 2 are associated with the photodetachment process leaving the He atom in the ^3P state. Peak 3 corresponds to the photodetachment process leaving the He atom in the ^3S state.

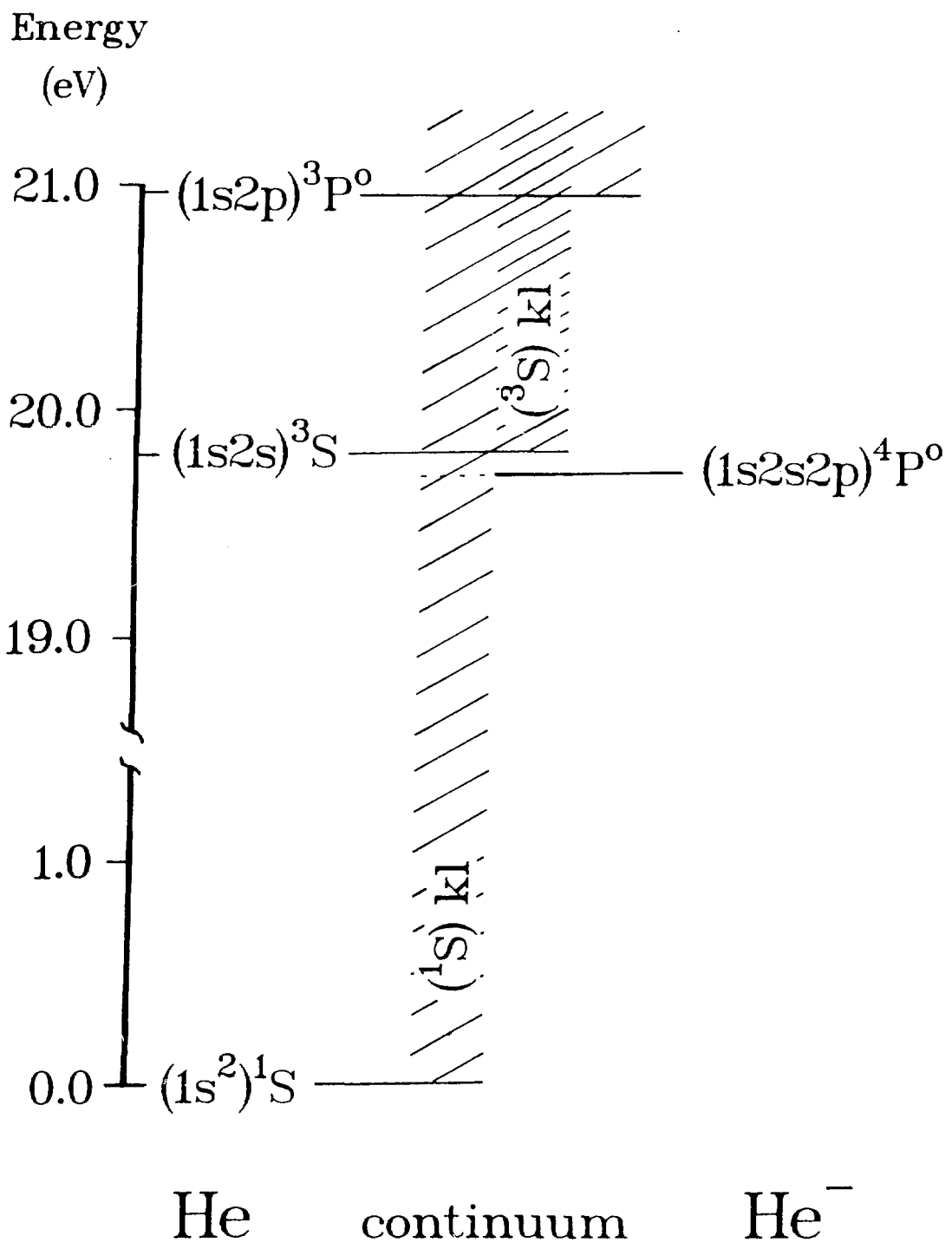
Energy
(eV)
21.0
20.0
19.0
1.0
0.0
$(1s2p)^3P^o$
$(1s2s)^3S$
$(1s^2)^1S$
(^3S) kl
(^1S) kl
$(1s2s2p)^4P^o$
He
continuum
He^-

Fig. 1

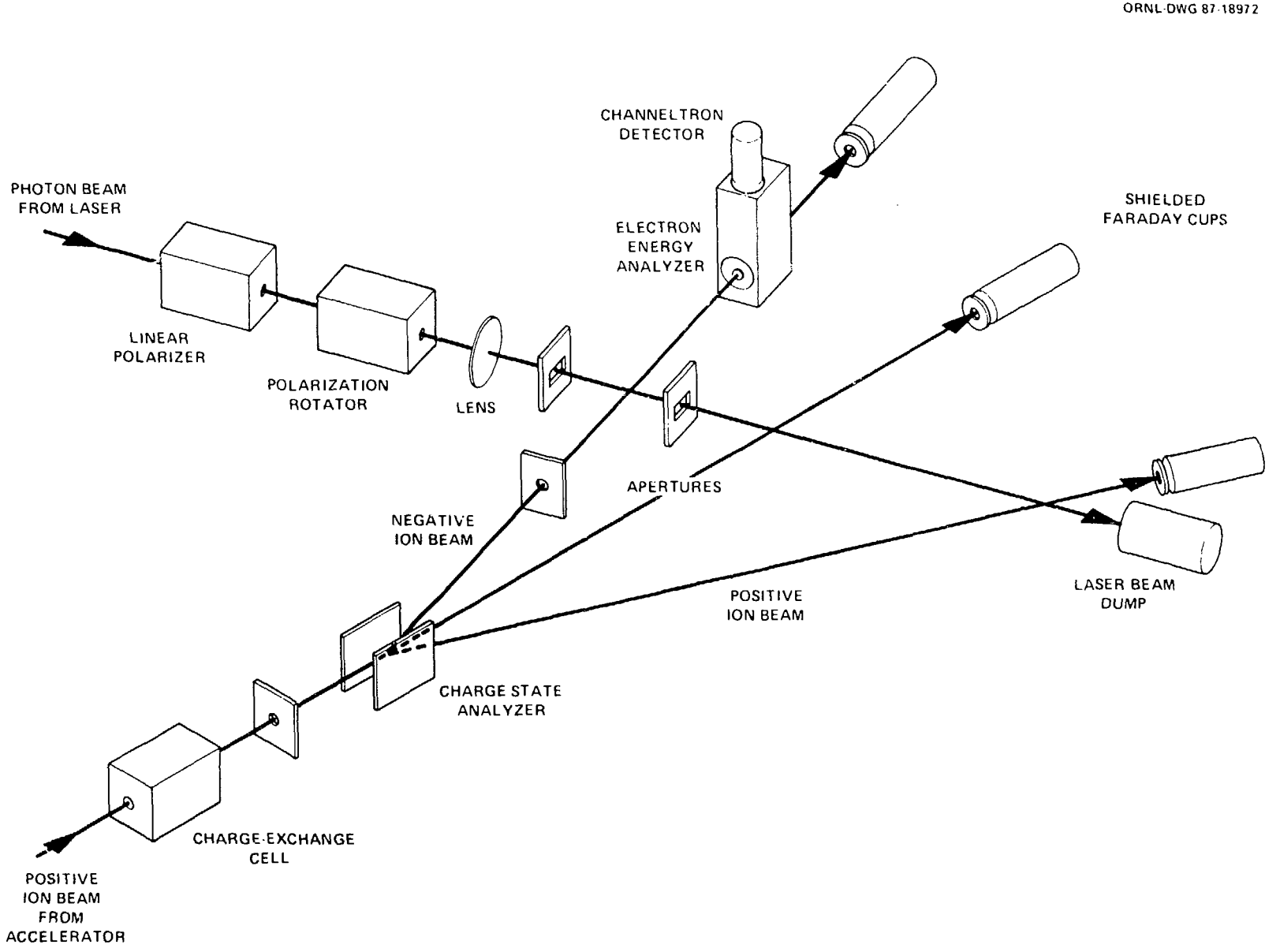
ORNL-DWG 87-18972
CHANNELTRON DETECTOR
PHOTON BEAM FROM LASER
ELECTRON ENERGY ANALYZER
SHIELDED FARADAY CUPS
LINEAR POLARIZER
POLARIZATION ROTATOR
LENS
APERTURES
NEGATIVE ION BEAM
LASER BEAM DUMP
POSITIVE ION BEAM
CHARGE STATE ANALYZER
CHARGE-EXCHANGE CELL
POSITIVE ION BEAM FROM ACCELERATOR

Fig. 2

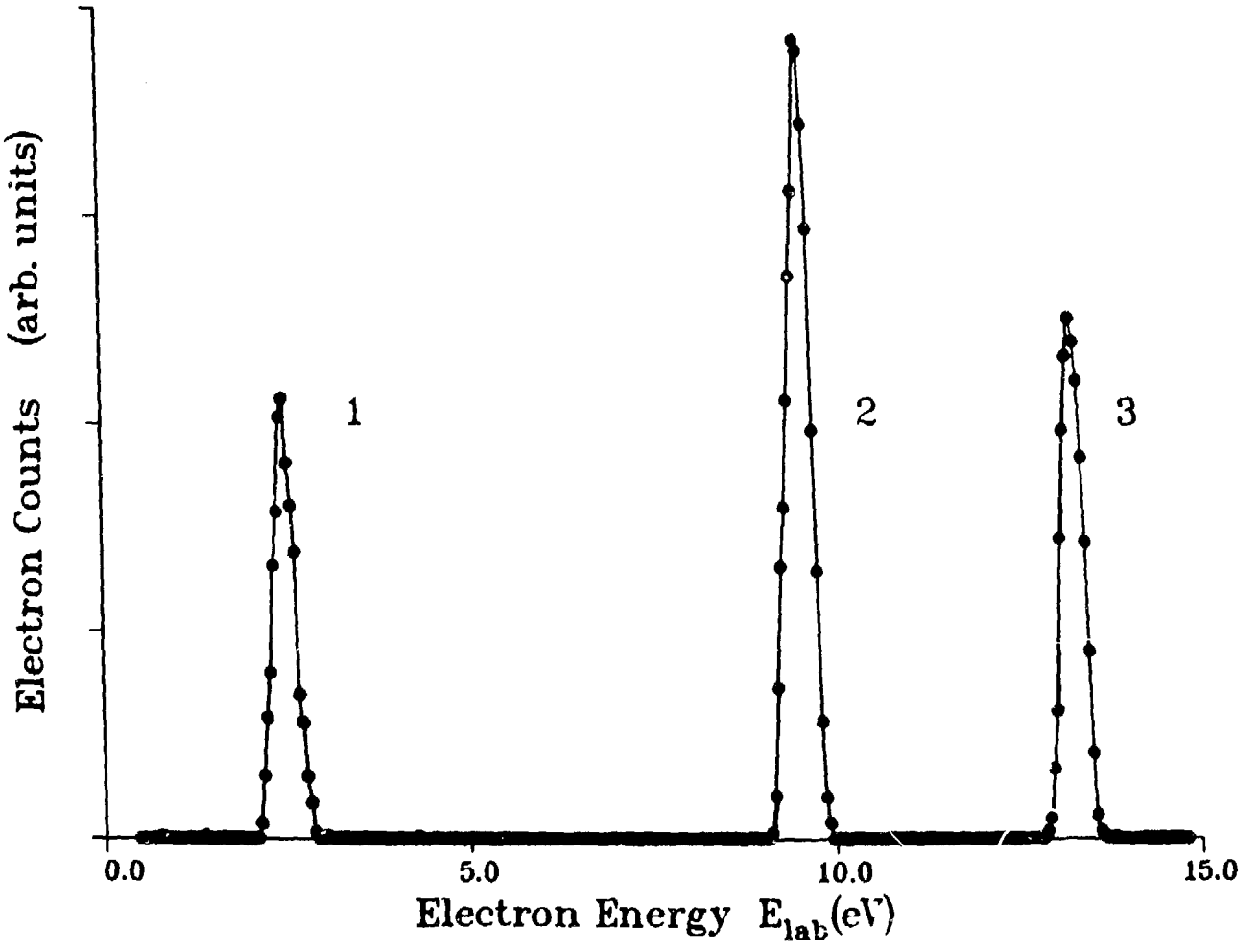
Photodetachment of He^- at 40 keV
λ=698.5 nm
Electron Counts (arb. units)
1
2
3
0.0
5.0
10.0
15.0
Electron Energy E_{lab}(eV)

Fig. 3